Fluorescent sensing platform for low-cost detection of Cu²⁺ by coumarin derivative: DFT calculation and practical application in herbal and black tea samples

Tahir SAVRAN[1] , **Abdurrahman KARAGÖZ**[1] , **Şükriye Nihan KARUK ELMAS**[1] ,
Duygu AYDIN[1] , **Furkan ÖZEN**[2] , **Kenan KORAN**[3] , **Fatma Nur ARSLAN**[1] ,
Ahmet Orhan GÖRGÜLÜ[3] , **İbrahim YILMAZ**[1,*]

[1]Department of Chemistry, Kamil Özdağ Science Faculty, Karamanoğlu Mehmetbey University, Karaman, Turkey
[2]Department of Mathematics and Science, Faculty of Education, Akdeniz University, Antalya, Turkey
[3]Department of Chemistry, Faculty of Science, Fırat University, Elazığ, Turkey

Abstract: A fluorogenic probe based on a coumarin-derivative for Cu²⁺ sensing in CH_3CN/H_2O media (v/v, 95/5, 5.0 µM) was developed and applied in real samples. 3-(4-chlorophenyl)-6,7-dihydroxy-coumarin (MCPC) probe was obtained by synthetic methodologies and identified by spectral techniques. The probe MCPC showed remarkable changes with a "turn-off" fluorogenic sensing approach for the monitoring of Cu²⁺ at 456 nm under an excitation wavelength of 366 nm. The response time of the probe MCPC was founded as only 1 min. The detection limit of the probe MCPC was recorded to be 1.47 nM. The binding constant and possible stoichiometric ratio (1:1) values were determined by Benesi-Hildebrand and Job's plot systems, respectively. The mechanism of the probe MCPC with Cu²⁺ was further confirmed by ESI-MS and FT-IR analyses, as well as supported by theoretical calculations. Furthermore, the probe MCPC was successfully employed for the practical applications to sense Cu²⁺ in different herbal and black tea samples. The proposed sensing method was also verified by ICP-OES method.

Key words: Coumarin, fluorescent sensor, copper, DFT, tea samples

1. Introduction

The rapid industrialization has caused heavy metal pollution which is gradually becoming a critical issue over the past three decades. This pollution is considered as a major threat, because heavy metal ions lead to serious problems for the ecological environment and human health [1]. Among the commonly encountered heavy metals of concern, the Cu²⁺ is the third most plentiful trace cation in the clay as well as in numerous livings, and it acts an essential role in numerous biological reactions. Cu²⁺ acts a vital role in the connective tissue growth, bone and blood formation as one of the physiological processes of organisms [2], it is also placed in the cornea and mostly in the brain [3]. However, it has been reported that excess intake of Cu²⁺ causes adverse health effects in the body such as gastrointestinal diseases and it damages the kidneys and liver [1,4]. Also, Cu²⁺ catalyzes the creation of reactive oxygen species which can harm basic biological molecules. According to various literatures, the toxicity of Cu²⁺ has linked to severe neurological diseases [5], Indian childhood cirrhosis (ICC) and prion diseases [2,4,6,7]. World Health Organization (WHO) has reported that the optimum intake of Cu²⁺ for adults

---

should not go above the level of 10–12 mg.day^{-1} [8]. For this reason, the monitoring of Cu^{2+} in a variety of drinking and food samples has been a vital issue for the protection of human health [7]. Thus, the development of reliable analytical procedures for Cu^{2+} sensing is still a critical research topic [9].

The reported methods for monitoring Cu^{2+} include inductively coupled mass-atomic emission spectrometry (ICM-AES), capillary electrophoresis (CE), atomic absorption spectrometry (AAS), voltammetry and inductively coupled plasma-mass spectrometry (ICP-MS) [10]. These techniques involve expensive analysis systems, troublous analysis procedures, and also need excessive use of samples [11]. In contrast, the fluorescence spectroscopy is currently taken into account as a powerful method for the recognition of Cu^{2+} owing to its real time, low cost, rapid and non destructive sensing with high selectivity and sensitivity [12] and easy operation. Recently, many fluorescent chemosensor studies for the recognition of Cu^{2+} have been reported [5,13,14]. To this end, various fluorescent probes based on rhodamine [15], naphthalene [16], BODIPY [17], fluorescein [18], N-aminophthalimide [19], thiophene [20], indole [21], pyrene [22], carbazole [23], cyanine [24] and coumarin [15] derivatives have employed to determine Cu^{2+} in several samples. Among these derivatives, coumarin-based molecules are powerful and highly adjustable fluorescent platforms for the selective and precise measurements of Cu^{2+} in drinking water, food and beverage samples [12].

Herein, a "turn-off" fluorogenic probe based on a coumarin-derivative, 3-(4-chlorophenyl)-6,7-dihydroxy-coumarin, probe MCPC, for Cu^{2+} sensing in CH_3CN/H_2O media (v/v, 95/5, 5.0 µM) was prepared and employed to various herbal and black tea samples. Coumarin compounds have been commonly used to be a florescent sensor thanks to its moderately high water solubility, high fluorescence quantum (Φ) yield and chemical stability, and also its large Stoke's shift. In addition, coumarin derivatives are less toxic to the livings and eco-friendly compounds [9]. The synthesized probe MPCP was successfully identified by spectral techniques such as ^{1}H-NMR and ^{13}C-ATP-NMR, as well as FT-IR. The theoretical computations were also done for the optimized geometric features.

2. Materials and methods

2.1. Chemicals and instrumentation

All chemicals used herein were of spectroscopic grade and obtained from Merck KGaA (Darmstadt, Germany) and VWR International B.V. (Amsterdam, Netherlands). Ultrapure water was acquired from Milli-Q$^{®}$7003/05/10/15 machine (Water purification system, Merck KGaA, Darmstadt, Germany). Solutions of different metal ions (Hg^{2+}, K^+, Mn^{2+}, Cu^{2+}, Ba^{2+}, Cd^{2+}, Co^{2+}, Ca^{2+}, Zn^{2+}, Mg^{2+}, Na^+, Fe^{2+}, Sr^{2+}, Pb^{2+}, Fe^{3+} and Al^{3+}) (10 mM, perchlorate salts in acetonitrile) were prepared as a stock solution.

A Bruker DPX 400 MHz spectrometer (Bruker Corp., Billerica, MA, USA) was employed to measure ^{13}C-APT-NMR and ^{1}H-NMR spectra. A Mass spectrometer (Bruker Daltonics-Microflex^{TM}, Bruker Corp.) was used to record electro spray ionization-mass spectra (ESI-MS). Infrared spectra were taken on a FT-IR spectrometer (Spectrum 100, Perkin Elmer Inc., Wellesley, MA, USA). A fluorescence spectrophotometer (Cary Eclipse, Agilent Tech., Santa Clara, CA, USA) was employed to record fluorescence spectra at rt. As a reference method, the amount of Cu^{2+} in herbal tea samples was analyzed by an inductively coupled plasma-optical emission spectroscopy (ICP-OES) (720, Agilent Tech.). For the pH measurements and centrifugation procedures, a pH meter (Mettler Toledo, Zaventem, Netherlands) and Universal 320R centrifuge system (Andreas Hettich GmbH & Co. KG, Tuttlingen, Germany) were used, respectively.

2.2. Fabrication of the probe MCPC

Probe MCPC, 6,7-dihydroxy-3-(4-chlorophenyl)coumarin, was successfully synthesized under microwave irradiation procedure with solvent free conditions according to the reported method in the literatures [25–27]. The synthesis protocols and characterization data were presented in Supplementary Information file in detail.

2.3. Fluorescence spectroscopic studies of the probe MCPC towards Cu^{2+} sensing

Probe MCPC was dissolved in acetonitrile as a stock solution and 10 mM of this was adjusted to 5.0 µM concentration with the mixture of CH_3CN/H_2O (v/v, 95/5). The titration experiments were performed to achieve the relationship between emission intensities and Cu^{2+}. For the fluorescence titration experiments, the different amounts of the cations (0–3.0 equiv) were added to 3000 µL of the probe solution. Spectra were taken at room temperature and recorded at $\lambda_{em} = 456$ nm ($\lambda_{ex} = 366$ nm, 5 nm slit width).

The LOD of the probe MCPC was calculated from the equation of $3\sigma/k$ (slope value) [28–31]. To analyze the effect of the possible competing cations on the sensing ability of probe MCPC to Cu^{2+}, suitable concentration of Cu^{2+} (3.0 equiv) was added into probe MCPC solution to generate MCPC-Cu^{2+} complex, afterwards each of the other cation solutions was added into the MCPC-Cu^{2+}, respectively. The emission intensities of the MCPC-Cu^{2+} complex were measured before and after adding other cations. The possible stoichiometric ratio between the probe MCPC and Cu^{2+} in MCPC-Cu^{2+} system was found by using Job's method calculation [32].

2.4. Studies based on DFT

Theoretical calculations were performed for the probe MCPC and MCPC-Cu^{2+} complex by the DFT / B3LYP/6-31 g (d) method with Gaussian 09 software (Gaussian, Inc., Wallingford, CT, UK) and accompanying graphical interface program GaussView 5.0.8 [33–37]. The LanL2DZ basis set for the effective potential set for Cu, and the 6-311G basis set was used for C, H, O atoms. To obtain the HOMO and LUMO energy levels, DFT analyses were performed based on the optimized geometries.

2.5. Detecting Cu^{2+} in tea samples by fluorometric sensing and ICP-OES

Eleven kinds of herbal tea leaves (green tea, white tea, sage tea, fennel tea, daisy tea, rose hip tea, ginger tea, mint tea, apple tea, linden tea and green tea mixture with rose) and 5 kinds of black tea leaves (black tea samples without aroma and black tea samples with bergamot aroma) were bought from super markets and herbs shops. 2.0 g of each samples were homogenized, individually placed into the boiled ultrapure water (50.0 mL) and infused/waited approximately for 15 min. Prepared tea solutions were placed in a shaker for 20 min, and then they were centrifuged at 10.000 rpm for 5 min. Final solutions were cleaned with a membrane filter (0.45 μm pore-size) and then the amounts of Cu^{2+} in teas were identified by the probe MCPC and ICP-OES systems. For fluorometric sensing analysis, probe MCPC solution was freshly prepared in CH_3CN/H_2O media (v/v, 95/5, 5.0 µM). 3000 µL of probe MCPC solution was put into the quartz-cuvette, and then the spectra were measured at rt ($\lambda_{ex} = 366$ nm, $\lambda_{em} = 456$ nm, 5 nm slit width). Then, 15 μL of each tea samples individually put into the probe MCPC, and the spectra were recorded by the same procedure. Finally, this solution (tea sample + probe MCPC) was spiked with 15 µL of diverse amounts of Cu^{2+} (0.1 and 0.2 μM) (standard addition method) and spectra were obtained. For ICP-OES analysis, the solution of tea samples were

acidified with HNO_3 (v/v, 1%) in the 10 mL of centrifuge tubes. pH value of these solutions were adjusted to 9 with a buffer solution (NH_3/NH_4Cl), and just after 15 min of waiting time, all teas were centrifuged at 10.000 rpm (~5 min). 0.5 mL of d-HNO_3 solution was added to the bottom layer in the tubes and this layer was diluted to 2500 µL with ultra-pure water. Before ICP-OES analysis, the sample solution was cleaned with a membrane filter (0.45 μm pore-size) to eliminate possible contaminations. The operating conditions of ICP-OES method were presented in Table S1. The analyses were done in triplicate and outcomes were illustrated as mean ±std.

3. Results and discussion

3.1. Design of the probe MCPC

The probe MCPC was prepared under microwave irradiation with solvent free condition by the reaction of compound **(3)** with pyridinium hydrochloride (85% yield) (Scheme 1), and it was well-verified by ^{1}H-NMR, FT-IR and ^{13}C-ATP-NMR analyses (Figures S1–S6).
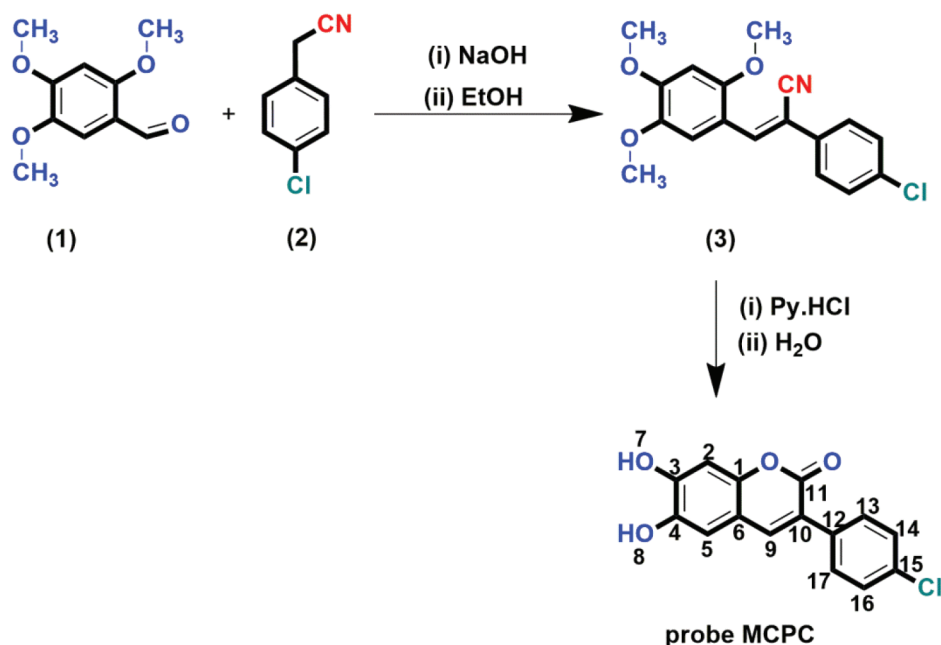

Scheme 1. Synthetic scheme of the probe MCPC.

As seen in FT-IR spectrum of the probe MCPC, the peaks appeared at 3197 and 3398 cm^{-1} were revealed the presence of -OH and also, -C = O peak in the coumarin ring was appeared at 1660 cm^{-1} (Figure S4). Moreover, the proton NMR for 2, 5, and 9 protons gives singlet peaks at 6.80, 7.08, and 8.16 ppm, respectively. In addition, protons 13 and 14 give doublet peaks at 7.51 and 7.74 ppm. The -OH proton peaks are observed at 9.56 and 10.34 ppm belong to H^7 and H^8. Characteristic functional group conversions show that the formation of probe MCPC was successfully achieved.

3.2. Fluorogenic response of the probe MCPC towards Cu^{2+} sensing

To study the fluorogenic sensing ability, the response of probe MCPC towards a series of various cations (Hg^{2+}, K^+, Mn^{2+}, Cu^{2+}, Ba^{2+}, Cd^{2+}, Co^{2+}, Ca^{2+}, Zn^{2+}, Mg^{2+}, Na^+, Fe^{2+}, Sr^{2+}, Pb^{2+}, Fe^{3+} and Al^{3+}) was

investigated in CH_3CN/H_2O media (v/v, 95/5, 5.0 µM) (Figure 1). The sensing property of probe MCPC was tested in the presence of possible competing ions at a fluorescence emission wavelength of 456 nm. As illustrated in Figure 1, only Cu^{2+} caused a diverse intensity change and emission intensity decreased sharply, whereas the probe MCPC did not give fluorogenic response towards other cations. None of the other cations caused remarkable impact on the intensity of probe MCPC. The probe MCPC exhibited only a small intensity change in the presence of Al^{3+} and Fe^{3+}. Thus, we concluded that the probe MCPC has good selectivity toward Cu^{2+} compared to other potential cationic species.
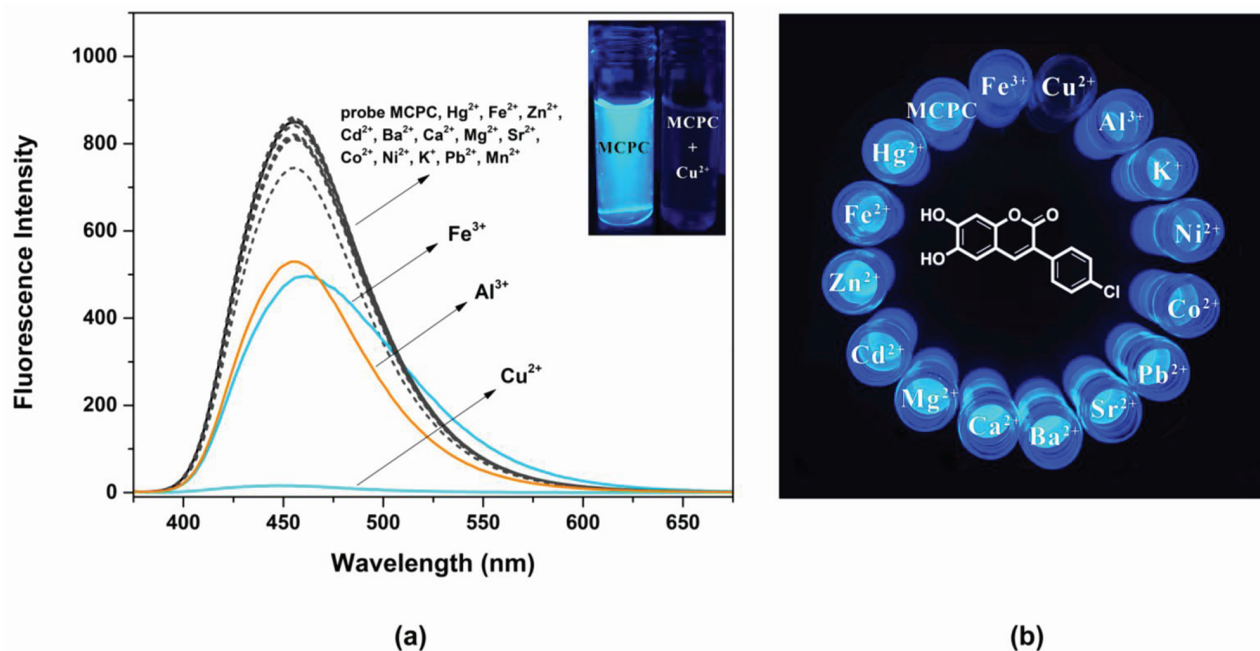
Figure 1. (a) Spectra of probe MCPC in the presence of competing ions (3.0 equiv), and (b) fluorescence colors of MCPC in presence of competing cations in CH_3CN/H_2O media (v/v, 95/5) (5.0 µM) ($\lambda_{ex} = 366$ nm, $\lambda_{em} = 456$ nm).

3.2.1. Competitive experiments

To determine the practical efficacy of probe MCPC as a fluorogenic chemosensor for Cu^{2+} monitoring, the competitive experiments were performed with various cations (3.0 equiv) (Hg^{2+}, K^+, Mn^{2+}, Cu^{2+}, Ba^{2+}, Cd^{2+}, Co^{2+}, Ca^{2+}, Zn^{2+}, Mg^{2+}, Na^+, Fe^{2+}, Sr^{2+}, Pb^{2+}, Fe^{3+} and Al^{3+}) in CH_3CN/H_2O media (v/v, 95/5, 5.0 µM) (Figure 2).

The emission intensity of probe MCPC was quenched with Cu^{2+} in the presence of other ions and there was no interference with other cations except Fe^{3+} (Figure 2). This cation could be easily masked by potassium thiocyanate (KSCN); hence it has a little impact on the selectivity of probe MCPC toward Cu^{2+}. That is to say, probe MCPC could be employed as an excellent selective sensor for the monitoring of Cu^{2+}.

3.2.2. Sensivity experiments

Fluorescence titration study was performed to investigate the quantitative interaction features of probe MCPC toward Cu^{2+} (Figure 3). Upon the adding of Cu^{2+} (0 to 3.0 equiv), probe MCPC showed a gradual emission
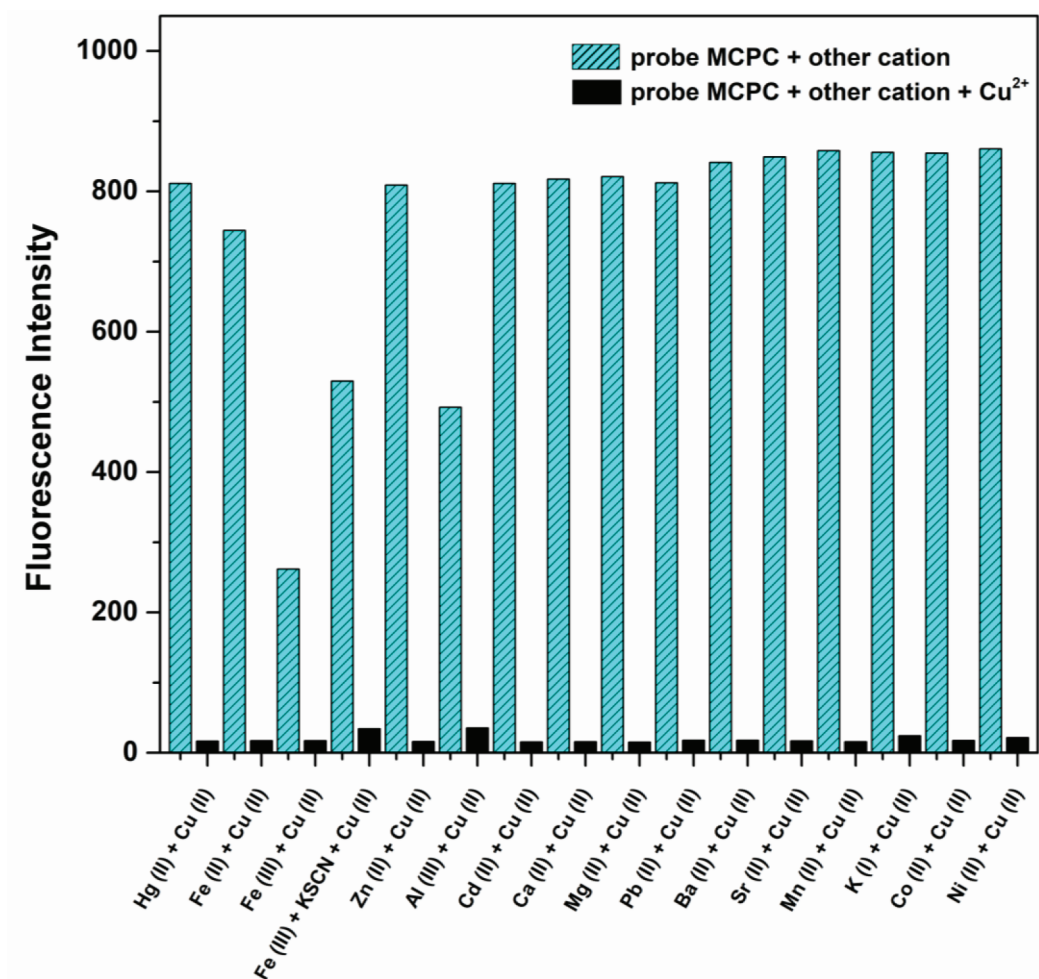
**Figure 2**. Competitive selectivity of probe MCPC (5.0 μM) toward Cu^{2+} in the presence of competing ions in CH_3CN/H_2O media (v/v, 95/5, 5.0 µM) (3.0 equiv, λ_{ex} = 366 nm, λ_{em} = 456 nm).

decreasement up to the constant equiv value, 3.0 equiv. Due to the complexation reaction between the probe MCPC and Cu^{2+}, the quenching phenomena could occur via the heavy atom & paramagnetic effect [38] and CHEQ (chelation enhancement quenching effect) [39] mechanisms. Therefore, the probe MCPC could be used as an outstanding "turn-off" fluorogenic sensor for Cu^{2+} monitoring.

3.2.3. Response time experiments

As well, the time dependence of the probe MCPC (5.0 μM) to Cu^{2+} (3.0 equiv) was studied (Figure S7) in CH_3CN/H_2O media (v/v, 95/5, 5.0 µM) to decide the reaction time for the MCPC-Cu^{2+}. The intensity of probe MCPC reached a maximum/stabile value within approximately 1 min; hence this result showed that probe **MCPC** could be used as a fluorogenic chemosensor for the rapid sensing of Cu^{2+}.
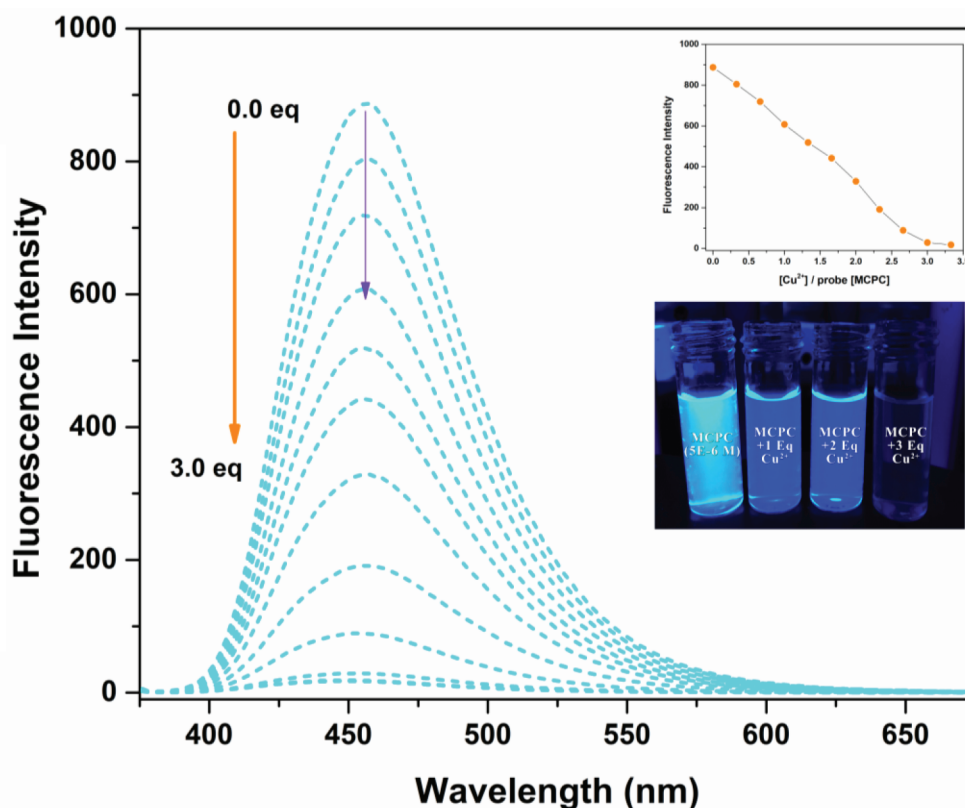
Figure 3. Spectral changes of probe MCPC upon the adding of Cu^{2+} (0 to 3.0 equiv) in CH_3CN/H_2O media (v/v, 95/5, 5.0 µM) (λ_{ex} = 366 nm, λ_{em} = 456 nm).

3.2.4. ESI-MS and Job's plot results

To consider the binding mode/stoichiometry of probe MCPC toward Cu^{2+}, Job's plot [32] (Figure 4), as well as ESI-MS analysis recorded in different matrixes and modes (Figures 5a and 5b) were carried out. The results of these analyses showed the stoichiometric ratio of MCPC-Cu^2+ complex as 1:1.

As illustrated in Figure 5, the peaks at 288.00 [m/z], 351.50 [m/z] and 367.50 [m/z] can be attributed to [probe MCPC], [probe MCPC + Cu^{2+}] and [probe MCPC + Cu^{2+}+ H_2O - 2•H^+], respectively, which demonstrated that probe MCPC complexed with Cu^{2+} in a ratio of 1:1. The content of water in the MCPC-Cu^{2+} system can be seen from the ESI-MS, as well from FT-IR spectrum (Figure S8). The complexation process was recognized between Cu^{2+} and two protons belong to the hydroxyl groups (Scheme 2).

On the basis of 1:1 stoichiometry, the binding constant of the MCPC-Cu^{2+} system was computed from the Benesi-Hildebrand equation [40], and it was found to be 1.23 $\times 10^4$ M^{-1}, which inferred that the stability of MCPC-Cu^{2+} complex was very high (Figure 6a). The calibration curve of the quantitative association between the intensity and amount of Cu^{2+} was acquired with an excellent linear range (y = 5.92 $\times 10^7$ x − 905.04, R^2 = 0.9957) at nanomolar levels (Figure 6b). The detection limit value of probe MCPC for Cu^{2+} was calculated as 1.47 nM (3σ / slope) [28,29]. The sensing properties of the probe MCPC are comparable to those of other reported literatures which are include cumarin-based fluorescent probes for Cu^{2+} (Table 1). When this study is
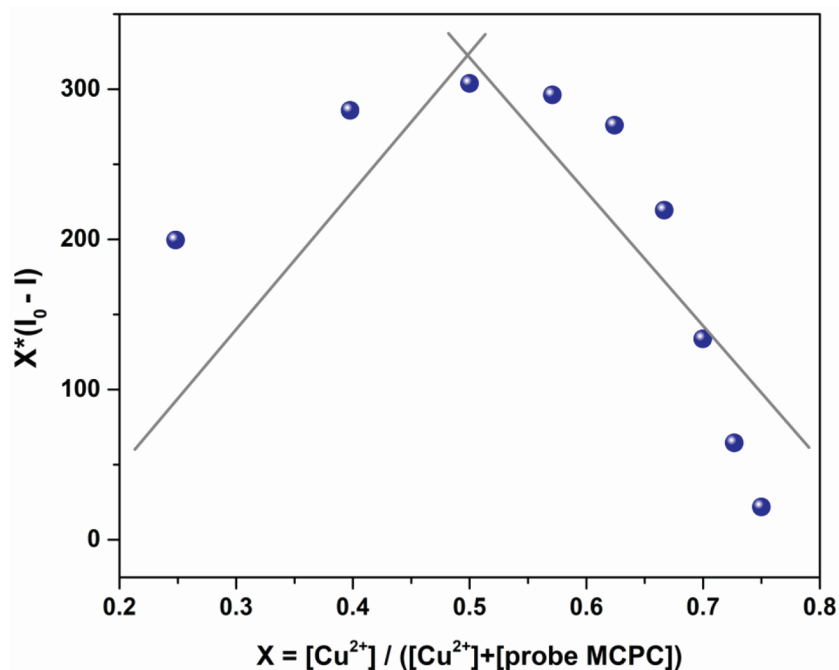
Figure 4. Job's plots of MCPC-Cu^{2+} complex in CH_3CN/H_2O media (v/v, 95/5, 5.0 µM) ($\lambda_{ex} = 366$ nm, $\lambda_{em} = 456$ nm).
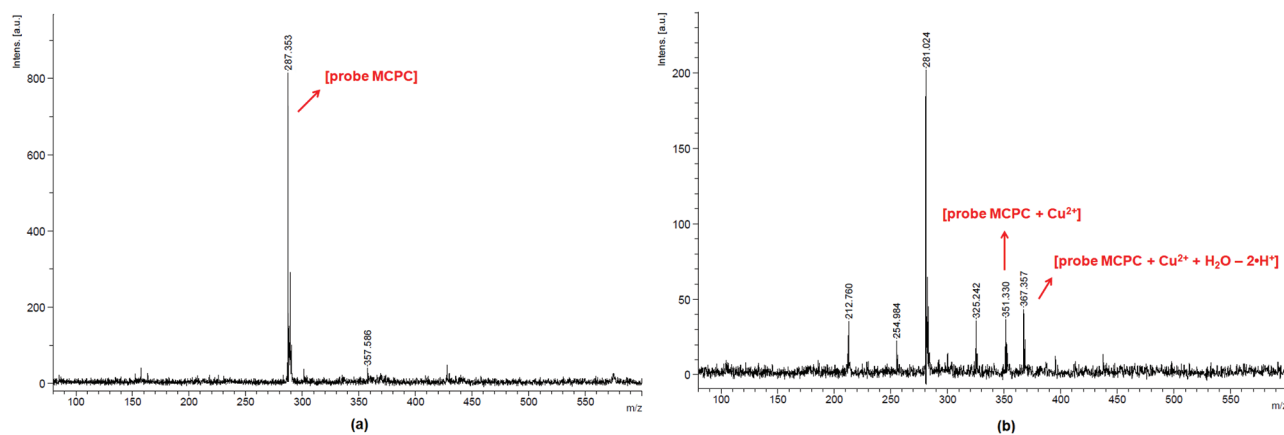
**Figure 5**. ESI-MS spectra of the probe MCPC and MCPC-Cu^{2+} system.

compared to our previous coumarin based fluorescent sensor studies [9,12], it is obvious that this study is more sensitive than others in terms of the detection limit value as a result of the substituent effect in the structure. Although the flour atom in the previous study is attached to the benzene ring through an aliphatic carbon, the chlorine in this study is directly connected to the benzene and has greater ability to attract the shared pair of electrons. Therefore, the acidic behaviors of the hydrogen of hydroxyl group increases, since chlorine in benzene ring demonstrates as well as resonance and inductive effect withdraws electrons while the delocalization of lone pair supplies electron density towards the ring. This system enables us the usability of this sensor for sensing of the toxic Cu^{2+} at lower concentrations. The electron-donating ability of F_3C^-, H_3C^-, Cl^- is examined,
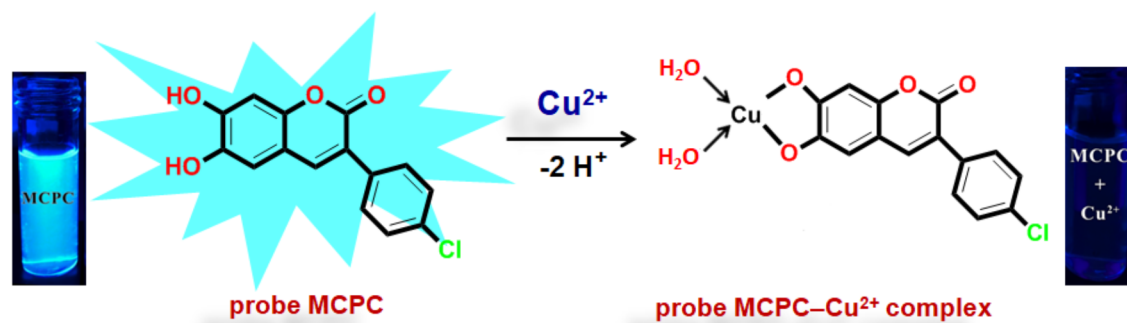
Scheme 2. Possible binding mechanism of the probe MCPC upon adding of Cu^{2+}.

it is found that $F_3C^- < H_3C^- < Cl^-$ and the abilities are directly proportional to the obtained detection limit values (24.5 nM <5.13 nM <1.47 nM). As a consequence, the obtained results showed that the probe MCPC had an excellent sensitivity toward Cu^{2+} sensing, as well as a good linearity for quantitative detections.
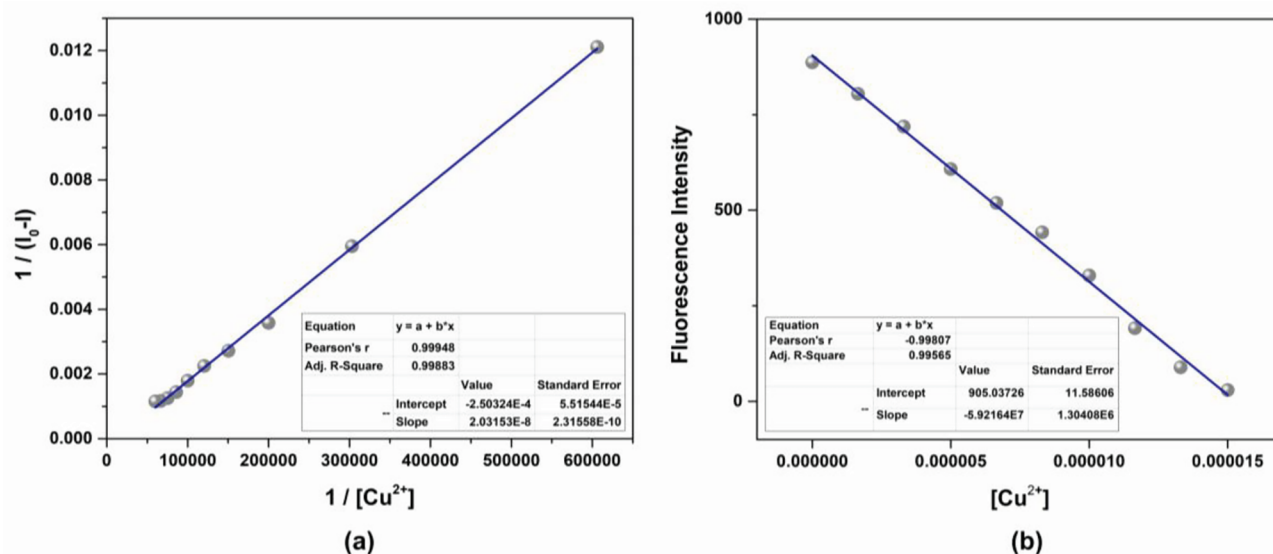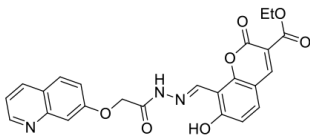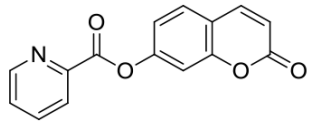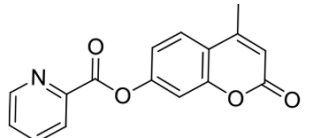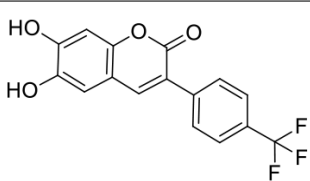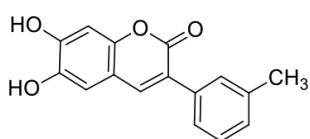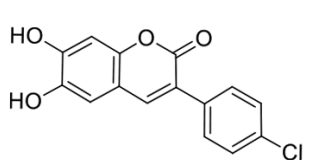

Figure 6. (a) Benesi-Hildebrand curve of $1/[Cu^{2+}]$ vs $1/(I-I_0)$, and (b) the calibration curve of the quantitative association between the intensities of probe MCPC and the amount of Cu^{2+} ($\lambda_{ex} = 366$ nm, $\lambda_{em} = 456$ nm).

3.3. DFT calculations of the probe MCPC and MCPC-Cu^{2+} complex

To determine the fluorometric sensing mechanism of probe MCPC binding to Cu^{2+}, theoretical computations were done by using the DFT / B3LYP/6-31 g (d,p) method with Gaussian-09 software package with and accompanying graphical interface program GaussView 5.0.8 [33–37]. The LanL2DZ basis set for the effective potential set for Cu, and the 6-311G basis set was employed for C, H, O atoms (Figure 7). The geometric optimizations were performed in the excited states to obtain the energy minimized structures of probe MCPC and MCPC-Cu^{2+} complex. As presented in Figure 7, the energy gap (ΔE) of probe MCPC was calculated to be 3.80 eV, and after Cu^{2+} addition, the ΔE decreased remarkably to 1.30 eV. We offered the stability of

Table 1. Relative work of the sensing performance of the probe **MCPC** with some coumarin-based probe studies.

| Probe	Solvent system	LOD (M)	Binding constant (Ka, 1/M)	Sample application	Ref.
	Na$_2$HPO$_4$-citric acid buffer (10 mmol/L)	256.00 $\times 10^{-9}$	1.75 $\times 10^6$	Yes	[41]
	Buffered water solution (10 mM Tris-HCl, containing 1% DMSO)	35.00 $\times 10^{-9}$	-	Yes	[42]
	PBS buffer solution /DMSO (v/v, 3/1)	62.00 $\times 10^{-9}$	-	Yes	[10]
	CH$_3$CN/H$_2$O (v/v, 95/5)	24.50 $\times 10^{-9}$	9.00 $\times 10^4$	Yes	[9]
	CH$_3$CN/HEPES (v/v, 95/5)	5.13 $\times 10^{-9}$	8.80 $\times 10^5$	Yes	[12]
	CH$_3$CN/H$_2$O (v/v, 95/5)	1.47 $\times 10^{-9}$	1.23 $\times 10^4$	Yes	this work

MCPC-Cu^{2+} complex was better than probe MCPC based on the theoretical calculations. The increase in the stability indicates that the route of the reaction tends to the formation of MCPC-Cu^{2+} complex, and therefore the fluorescence quenching occurs.

3.4. Fluorometric sensing and ICP-OES analysis of the tea samples

To assess the potential usage of probe MCPC for practical applications, Cu^{2+} levels were measured in various herbal tea samples, as well as black tea samples (Table 2). The samples were analyzed by the calibration plot (Figure 6b) of the emission intensities of probe MCPC toward Cu^{2+}. A standard addition method was also
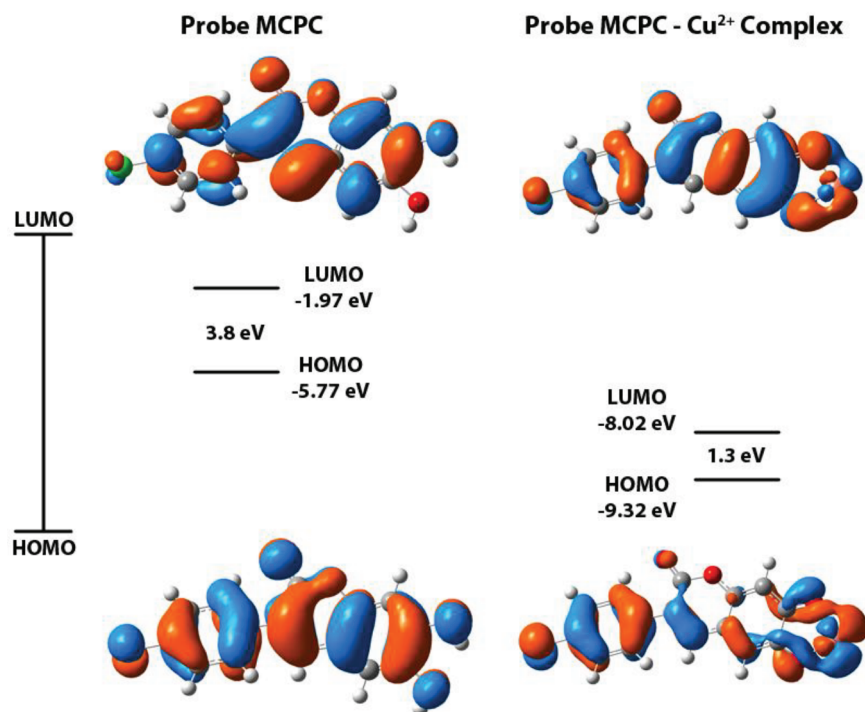
Figure 7. Energy level diagrams of the MCPC-Cu^{2+} complex and probe MCPC.

employed by adding two different concentrations (0.1 and 0.2 μmol L^{-1}) of Cu^{2+} into the tea samples. As indicated in Table S2, probe MCPC could be very practical for Cu^{2+} sensing with satisfactory accuracy and precision values in tested tea samples. The fluorometric sensing method's recovery values were calculated within a range from 90.22% to 109.19%. Thus, Cu^{2+} can be identified with excellent recovery values in herbal and black tea samples.

Table 2. Determination of Cu^{2+} in herbal and black teas by ICP-OES and probe MCPC.

	Cu^{2+} (μmol.L^{-1})		Difference of the means	Statistics (df = 2)		
	MPCP	ICP-OES		t$_{Statistic}$	probability >|t|	
Herbal tea samples						
Green tea	0.1745 ±0.0021	0.1724 ±0.0017	0.0022	2.5476	0.1257	
Green tea (mixed with rose)	0.0244 ±0.0004	0.0254 ±0.0006	−0.0009	−1.8199	0.2104	
White tea	0.1267 ±0.0010	0.1276 ±0.0017	−0.0009	−1.2051	0.3514	
Sage tea	0.0689 ±0.0009	0.0682 ±0.0014	0.0006	1.3093	0.3206	
Fennel tea	0.0384 ±0.0004	0.0386 ±0.0007	−0.0001	−0.3780	0.7418	t $_{tabulated}$ >t $_{calculated}$
Daisy tea	0.0791 ±0.0008	0.0789 ±0.0010	0.0002	2.4277	0.1359	
Rose hip tea	0.0664 ±0.0010	0.0662 ±0.0012	0.0003	1.8898	0.1994	
Ginger tea	0.0222 ±0.0002	0.0221 ±0.0011	0.0002	0.3111	0.7852	
Mint tea	0.0851 ±0.0010	0.0855 ±0.0017	−0.0003	−0.4804	0.6784	
Apple tea	0.0104 ±0.0010	0.0102 ±0.0006	0.0002	0.5547	0.6348	
Linden tea	0.0880 ±0.0009	0.0876 ±0.0013	0.0004	0.7184	0.5471	
Black tea samples						
Black tea without aroma-A	0.0843 ±0.0010	0.0845 ±0.0022	−0.0002	−0.2857	0.8019	
Black tea without aroma-B	0.0165 ±0.0002	0.0169 ±0.0006	−0.0004	−1.7320	0.2254	
Black tea without aroma-C	0.0535 ±0.0004	0.0537 ±0.0013	−0.0002	−0.3255	0.7757	t $_{tabulated}$ >t $_{calculated}$
Black tea with bergamot aroma-A	0.1321 ±0.0009	0.1319 ±0.0031	0.0002	0.1644	0.8845	
Black tea with bergamot aroma-B	0.0506 ±0.0003	0.0522 ±0.0021	−0.0015	−1.4034	0.2956	

†mean(1)-mean(2) = 0 based on Null Hypothesis; mean(1)-mean(2) <>0 based on Alternative Hypothesis; the differentiation of the means is NOT considerably dissimilar with the test variation (0) (at the 0.05 level).

The validity of the proposed sensing method for Cu^{2+} detection was checked by employing ICP-OES analysis. Likewise the proposed fluorescence method, samples were spiked with recognized quantities of Cu^{2+} (0.01–0.02 mgL^{-1}) (Table S3). The calibration graphs were constructed for the determination of Cu^{2+} quantitatively (0.01–1.00 mgL^{-1}) by ICP-OES method. Recoveries of Cu^{2+} were between 94.58 and 105.66% values, and the good agreements were found between the obtained and added quantities of Cu^{2+}. The results of the fluorescence and atomic spectroscopy methods were compared (Table 2), and the differences of the means of two methods were not found significantly different from each others at the 0.05 level.

Conclusion

As a conclusion, we have developed a low-cost, highly selective and sensitive probe MCPC with quite-low detection limit for the fluorescent sensing of Cu^{2+}. Probe MCPC demonstrated excellent fluorescence "turn-off" response to Cu^{2+} in CH_3CN/H_2O media (v/v, 95/5, 5.0 µM) at 456 nm with emission quenching, and it revealed a rapid response time ($\sim$60 s). The detection limit was found as 1.47 nM according to 3σ/slope, which indicated excellent sensitivity to Cu^{2+} sensing in nanomolar levels. The ΔE values of the probe **MCPC** and its complex were calculated to be 3.80 eV and 1.30 eV, respectively. Studies on real samples, herbal and black teas, revealed that the probe **MCPC** can sensitively and selectively recognize Cu^{2+} with good recovery values (90.22%–109.19%). The outcomes of the probe MCPC and ICP-OES analyses were also compared and the differences of the means of two methods were not found significantly different (P <0.05). Thus, these promising findings could make a great contribution to researchers studying Cu^{2+} detection in different foodstuffs.

References

1. Wang S, Ding H, Wang Y, Fan C, Liu G et al. A colorimetric and ratiometric fluorescent sensor for sequentially detecting Cu^{2+} and arginine based on a coumarin-rhodamine B derivative and its application for bioimaging. RSC Advances 2019; 9 (12): 6643-6649. doi: 10.1039/c8ra09943j

2. Roy N, Nath S, Dutta A, Mondal P, Paul PC et al. A highly efficient and selective coumarin based fluorescent probe for colorimetric detection of Fe^{3+} and fluorescence dual sensing of Zn^{2+} and Cu^{2+}. RSC Advances 2016; 6 (68): 63837-63847. doi: 10.1039/c6ra12217e

3. Bekhradnia A, Domehri E, Khosravi M. Novel coumarin-based fluorescent probe for selective detection of Cu (II). Spectrochimica Acta Part A: Molecular and Biomolecular Spectroscopy 2016; 152 (1): 18-22. doi: 10.1016/j.saa.2015.07.029

4. Jung HS, Kwon PS, Lee JW, Kim JII, Hong CS et al. Coumarin-derived Cu^{2+}-selective fluorescence sensor: synthesis, mechanisms, and applications in living cells. Journal of the American Chemical Society 2009; 131 (5): 2008-2012. doi: 10.1021/ja808611d

5. Kim MH, Jang HH, Yi S, Chang SK, Han MS. Coumarin-derivative-based off-on catalytic chemodosimeter for Cu^{2+} ions. Chemical Communications 2009; 32 (1): 4838-4840. doi: 10.1039/b908638b

6. Shi Y, Wang R, Yuan W, Liu Q, Shi M et al. Easy-to-use colorimetric cyanine probe for the detection of Cu^{2+} in Wilson's disease. ACS Applied Materials & Interfaces, 2018; 10 (24): 20377-20386. doi: 10.1021/acsami.8b07081

7. Yeh JT, Chen WC, Liu SR, Wu SP. A coumarin-based sensitive and selective fluorescent sensor for copper(II) ions. New Journal of Chemistry 2014; 38 (9): 4434-4439. doi: 10.1039/c4nj00695j

8. Qian B, Váradi L, Trinchi A, Reichman SM, Bao L et al. The Design and synthesis of fluorescent coumarin derivatives and their study for Cu^{2+} sensing with an application for aqueous soil extracts. Molecules, 2019; 24 (19): 3569. doi: 10.3390/molecules24193569

9. Arslan FN, Geyik GA, Koran K, Ozen F, Aydin D et al. Fluorescence "turn on-off" sensing of copper (II) ions utilizing coumarin-based chemosensor: experimental study, theoretical calculation, mineral and drinking water analysis. Journal of Fluorescence 2020; 30 (1): 317-327. doi: 10.1007/s10895-020-02503-4

10. Wu X, Wang H, Yang S, Tian H, Liu Y et al. A novel coumarin-based fluorescent probe for sensitive detection of copper(II) in wine. Food Chemistry 2019; 284 (1): 23-27. doi: 10.1016/j.foodchem.2019.01.090

11. Yan F, Bai Z, Chen Y, Zu F, Li X et al. Ratiometric fluorescent detection of copper ions using coumarin-functionalized carbon dots based on FRET. Sensors and Actuators B: Chemical 2018; 275 (1): 86-94. doi: 10.1016/j.snb.2018.08.034

12. Karuk Elmas SN, Gunay IB, Koran K, Ozen F, Aydin D et al. An ultrasensitive and selective "turn off" fluorescent sensor with simple operation for the determination of trace copper (II) ions in water and various beverage samples. Supramolecular Chemistry 2019; 31 (12): 756-766. doi: 10.1080/10610278.2019.1702195

13. Aksuner N, Henden E, Yilmaz I, Cukurovali A. A highly sensitive and selective fluorescent sensor for the determination of copper (II) based on a schiff base. Dyes and Pigments 2009; 83 (2): 211-217. doi: 10.1016/j.dyepig.2009.04.012

14. Aksuner N, Henden E, Yilmaz I, Cukurovali A. Selective optical sensing of copper(II) ions based on a novel cyclobutane-substituted schiff base ligand embedded in polymer films. Sensors and Actuators B: Chemical 2008; 134 (2): 510-515. doi: 10.1016/j.snb.2008.05.041

15. Wang Y, Meng Q, Han Q, He G, Hu Y et al. Selective and sensitive detection of cysteine in water and live cells using a coumarin-Cu^{2+} fluorescent ensemble. New Journal of Chemistry 2018; 42 (19): 15839-15846. doi: 10.1039/c8nj03809k

16. Kumar A, Mondal S, Kayshap KS, Hira SK, Manna PP et al. Water switched aggregation/disaggregation strategies of a coumarin-naphthalene conjugated sensor and its selectivity towards Cu^{2+} and Ag^+ ions along with cell imaging studies on human osteosarcoma cells (U-2 OS). New Journal of Chemistry 2018; 42 (13): 10983-10988. doi: 10.1039/c8nj01631c

17. Zhang J, Zhao B, Li C, Zhu X, Qiao R. A BODIPY-based "turn-on" fluorescent and colorimetric sensor for selective detection of Cu^{2+} in aqueous media and its application in cell imaging. Sensors and Actuators B: Chemical 2014; 196 (1): 117-122. doi: 10.1016/j.snb.2014.01.116

18. Hormozi-Nezhad MR, Taghipour M. An ultrasensitive and selective turn-off fluorescent nanoprobe for the detection of copper ions. Analytical Methods 2015; 7 (12): 5067-5073. doi: 10.1039/c5ay00766f

19. Joo DH, Mok JS, Bae GH, Oh SE, Kang JH et al. Colorimetric detection of Cu^{2+} and fluorescent detection of PO_4^{3-} and S^{2-} by a multifunctional chemosensor. Industrial & Engineering Chemistry Research 2017; 56 (30): 8399-8407. doi: 10.1021/acs.iecr.7b01115

20. Guo Z, Hu T, Wang X, Sun T, Li T et al. Highly sensitive and selective fluorescent sensor for visual detection of Cu^{2+} in water and food samples based on oligothiophene derivative. Journal of Photochemistry and Photobiology A: Chemistry 2019; 371 (1): 50-58. doi: 10.1016/j.jag.2018.07.004

21. Chang Y, Li B, Mei H, Yang L, Xu K et al. Indole-based colori/fluorimetric probe for selective detection of Cu^{2+} and application in living cell imaging. Spectrochimica Acta Part A: Molecular and Biomolecular Spectroscopy 2020; 226 (1): 117631. doi: 10.1016/j.saa.2019.117631

22. Wu SP, Huang ZM, Liu SR, Chung PK. A pyrene-based highly selective turn-on fluorescent sensor for copper(II) ion and its application in live cell imaging. Journal of Fluorescence 2012; 22 (1): 253-259. doi: 10.1007/s10895-011-0955-7

23. Jiao X, Xiao Z, Hui P, Liu C, Wang Q et al. A highly selective and pH-tolerance fluorescent probe for Cu^{2+} based on a novel carbazole-rhodamine hybrid dye. Dyes and Pigments 2019; 160 (1): 633-640. doi: 10.1016/j.dyepig.2018.08.060

24. Li J, Ge J, Zhang Z, Qiang J, Wei T et al. A cyanine dye-based fluorescent probe as ındicator of copper clock reaction for tracing Cu^{2+}-catalyzed oxidation of cysteine. Sensors and Actuators B: Chemical 2019; 296 (1): 126578. doi: 10.1016/j.snb.2019.05.055

25. Özen F, Tekin S, Koran K, Sandal S, Görgülü AO. Synthesis, structural characterization, and in vitro anti-cancer activities of new phenylacrylonitrile derivatives. Applied Biological Chemistry 2016; 59 (1): 239-248. doi: 10.1007/s13765-016-0163-x

26. Buu-Hoi NP, Saint-Ruf G, Lobert B. Oxygen heterocycles. part XIV. hydroxylated 3-awl- and 3-pyridyl-coumarins. Journal of the Chemical Society C: Organic 1968; 16 (1): 2069-2070. doi: 10.1039/J39690002069

27. Elgazzar E, Dere A, Özen F, Koran K, Al-Sehemi AG et al. Design and fabrication of dioxyphenylcoumarin substituted cyclotriphosphazene compounds photodiodes. Physica B: Condensed Matter 2017; 515 (1): 8-17. doi: 10.1016/j.physb.2017.03.025

28. Aydin D. A novel turn on fluorescent probe for the determination of Al^{3+} and Zn^{2+} ions and its cells applications. Talanta 2020; 210 (1): 120615. doi: 10.1016/j.talanta.2019.120615

29. Qiu S, Cui S, Shi F, Pu S. Novel diarylethene-based fluorescent switching for the detection of Al^{3+} and construction of logic circuit. ACS Omega 2019; 4 (1): 14841-14848. doi: 10.1021/acsomega.9b01432

30. Karuk Elmas ŞN, Yilmaz I. A turn off-on fluorescent chemosensor for sequential determination of mercury and biothiols. Journal of Fluorescence 2018; 28 (1): 1451-1458. doi: 10.1007/s10895-018-2320-6

31. Karuk Elmas ŞN, Ozen F, Koran K, Görgülü AO, Sadi G et al. Selective and sensitive fluorescent and colorimetric chemosensor for detection of CO$_3^{2-}$ anions in aqueous solution and living cells. Talanta 2018; 188 (1): 614-622. doi: 10.1016/j.talanta.2018.06.036

32. Huang CY. Determination of binding stoichiometry by the continuous variation method: the Job plot. Methods in Enzymol 1982; 87 (1): 509-525. doi: 10.1016/S0076-6879(82)87029-8

33. Frisch AMJ, Trucks GW, Schlegel HB, Scuseria GE, Robb MA et al. Gaussian 09 Revision D.01. 2014.

34. Dennington R, Keith TA, Millam JM. GaussView Version 5. 2009.

35. Becke AD. Becke's three parameter hybrid method using the LYP correlation functional. The Journal of Chemical Physics 1993; 98 (1): 5648-5652. doi: 10.1063/1.464913

36. Lee C, Hill C, Carolina N. Development of the colic-salvetti correlation-energy formula into a functional of the electron density. Physical Review B 1988; 37 (2): 785-789. doi: 10.1103/PhysRevB.37.785

37. Hay PJ, Wadt WR. Ab initio effective core potentials for molecular calculations. potentials for the transition metal atoms Sc to Hg. The Journal of Chemical Physics 1985; 82 (1): 270-283. doi: 10.1063/1.448799

38. Yang S, Yin B, Xu L, Gao B, Sun H et al. A natural quercetin-based fluorescent sensor for highly sensitive and selective detection of copper ions. Analytical Methods 2015; 7 (1): 4546-4551. doi: 10.1039/C5AY00375J

39. Duarte LGTA, Coelho FL, Germino JC, Costa GG, Berbigier JF et al. A selective proton transfer optical sensor for copper II based on chelation enhancement quenching effect (CHEQ). Dyes and Pigments 2020; 108566. doi: 10.1016/j.dyepig.2020.108566 40. Hildebrand JH, Benesi HA. A spectrophotometric investigation of the interaction of iodine with aromatic hydrocarbons. Journal of the American Chemical Society 1949; 71 (8): 2703-2707. doi: 10.1038/164963b0

40. Duan YW, Tang HY, Guo Y, Song ZK, Peng MJ et al. The synthesis and study of the fluorescent probe for sensing Cu2+ 4 based on a novel coumarin Schiff-base. Chinese Chemistry Letters 2014; 25 (7): 1082-1086. doi: 10.1016/j.cclet.2014.05.001

41. Zhou Z, Li N, Tong A. A new coumarin-based fluorescence turn-on chemodosimeter for Cu^{2+} in water. Analytica Chimica Acta 2011; 702: 81-86. doi: 10.1016/j.aca.2011.06.041

MATERIALS AND METHODS

Microwave–assisted solvent free synthesis of probe MCPC

3.03 mmol Phenylacrylonitrile compound **(3)** [1–3] and pyridinium hydrochloride (5 g) were reacted in silica gel and the reaction mixture was subjected to microwave irradiation at 320 watt for 30 min. The reaction was quenched with 1.0 N HCl (200 mL) as soon as the reaction completed. The reaction mixture filtered, the residue dissolved in acetone (20 mL) four times and filtered over silica gel. The solvent was evaporated and the residue washed with water and then dried. The obtained solid was precipitated with ethyl acetate (15 mL) and n–hexane (250 mL). The obtained crude product was separated by column chromatography.

A fawn colored solid compound, probe **MCPC**, was obtained (0.75 g, 85%). Anal. Calc. for $C_{15}H_9ClO_4$ (MW: 288.68): C, 62.41; H, 3.14; Found C, 62.44, H; 3.17%. FT–IR (KBr, cm^{-1}): 3197, 3398ν_{O-H}, 3000–3090 $\nu_{C-H(Ar)}$, 1660 $\nu_{C=O}$, 1563, 1571, and 1621 $\nu_{C=C}$. ^{1}H NMR (400 MHz, DMSO–d$_6$): δ 6.80 (1H, s, H^2), 7.08 (1H, s, H^5), 7.51 (2H, d, J=8.4 Hz, H^{13}), 7.74 (2H, d, J=8.8 Hz, H^{14}), 8.16 (1H, s, H^9), 9.56 (1H, s, H^7), 10.34 (1H, s, H^8). ^{13}C–NMR (400 MHz, DMSO–d$_6$): δ 143.59 C^1, 102.69 C^2, 151.21 C^3, 148.65 C^4, 112.92 C^5, 111.88 C^6, 141.92 C^9, 121.27 C^{10}, 160.66 C^{11}, 132.97 C^{12}, 128.59 C^{13,17}, 130.48 C^{14,16}, and 134.63 C^{15}.

RESULTS AND DISCUSSION
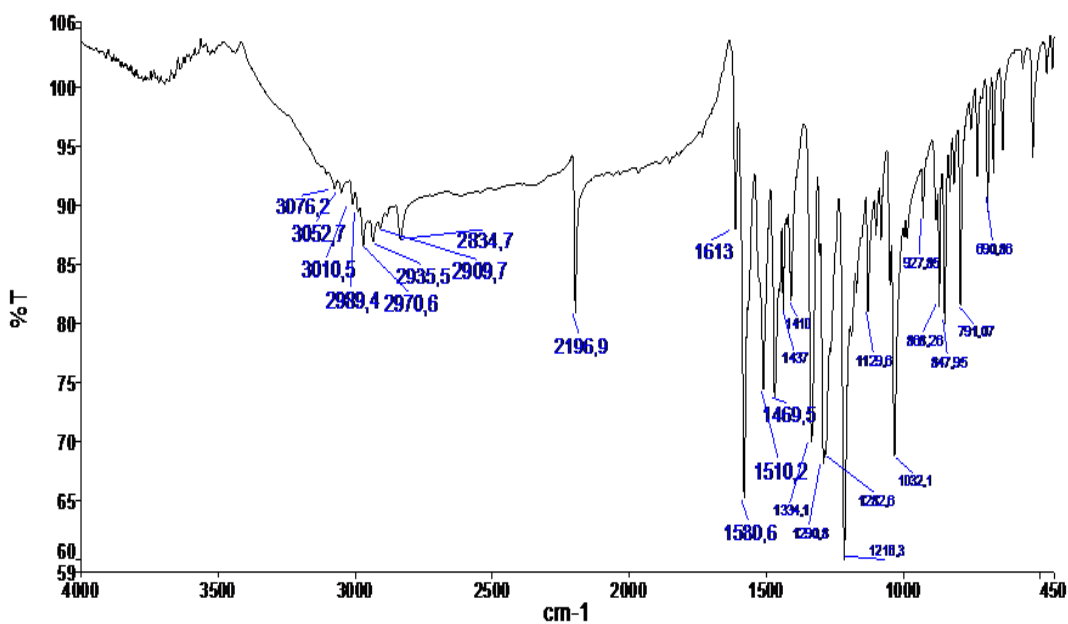
Figure S1. FT–IR spectrum of the compound **(3)**
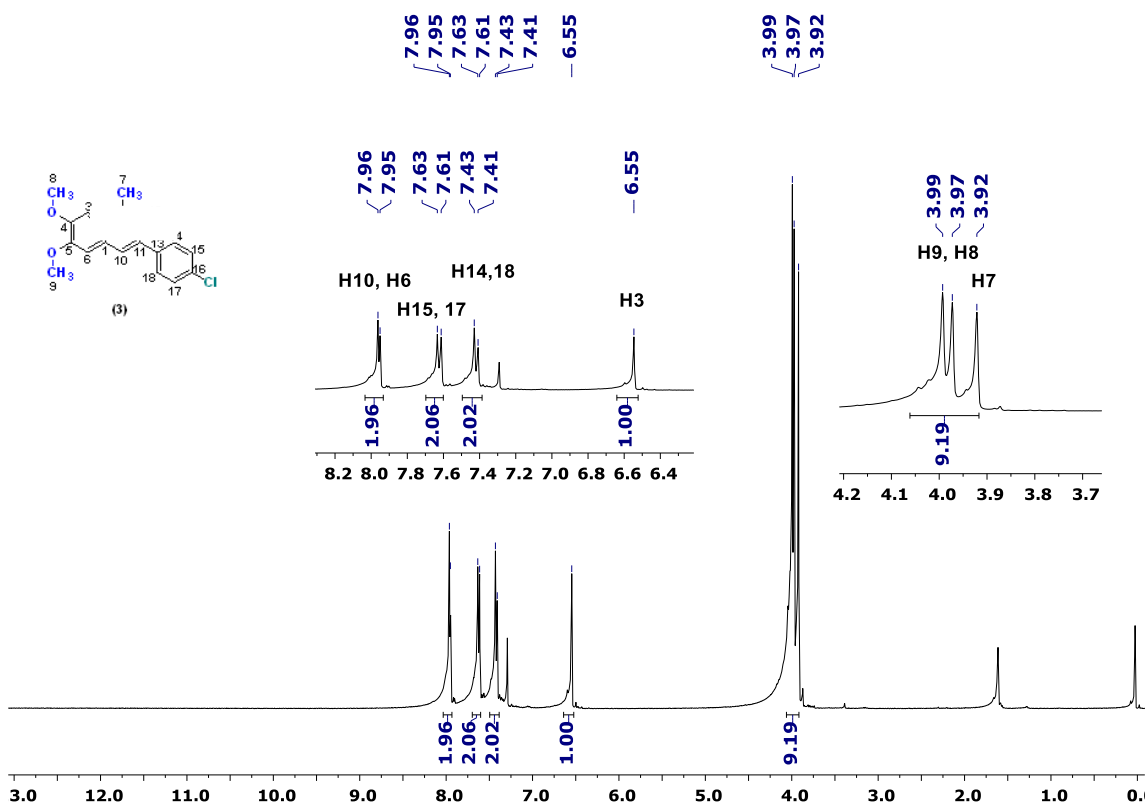
Figure S2. ^{1}H NMR spectrum of the compound **(3)** in CDCl$_3$–d_1
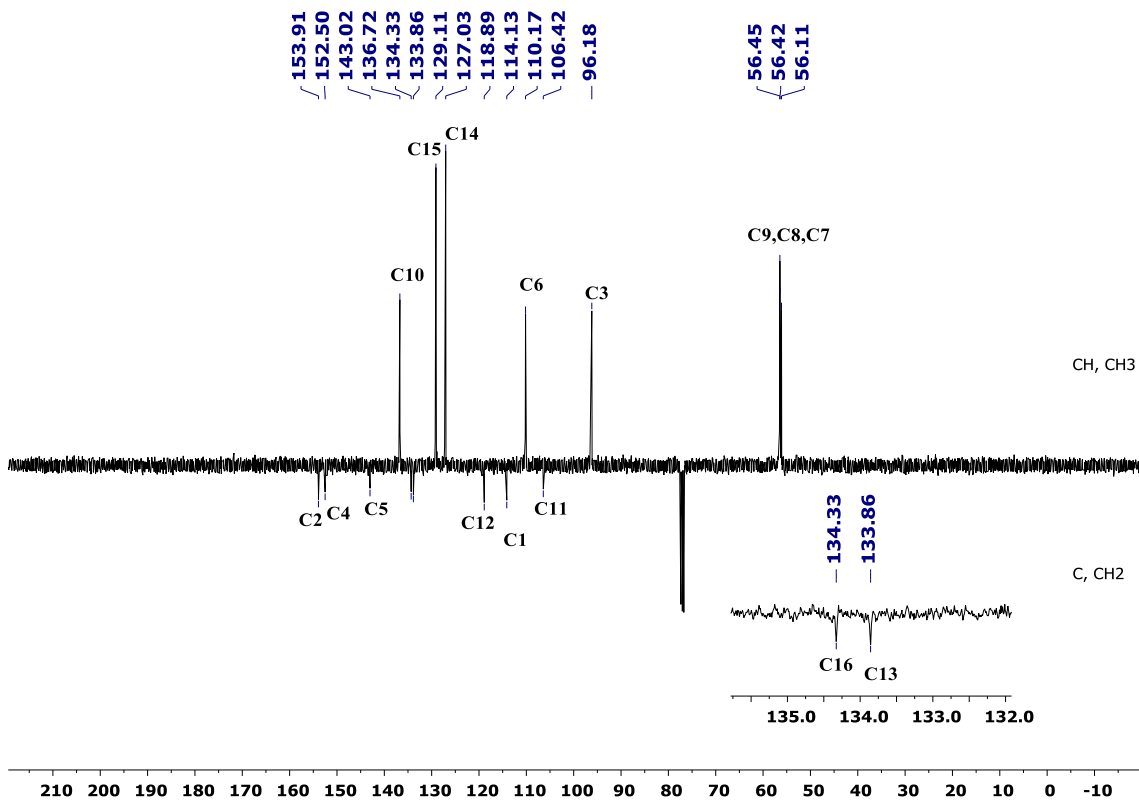
Figure S3. ^{13}C–APT NMR spectrum of the compound **(3)** in CDCl$_3$–d_1
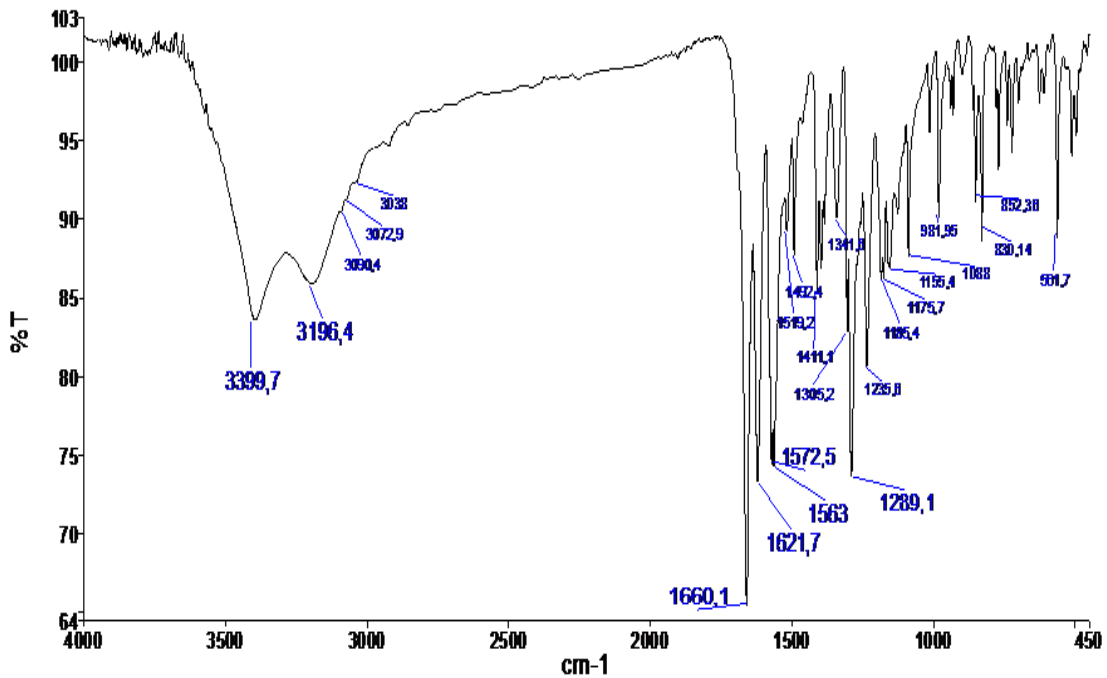
Figure S4. FT–IR spectrum of the probe **MCPC**
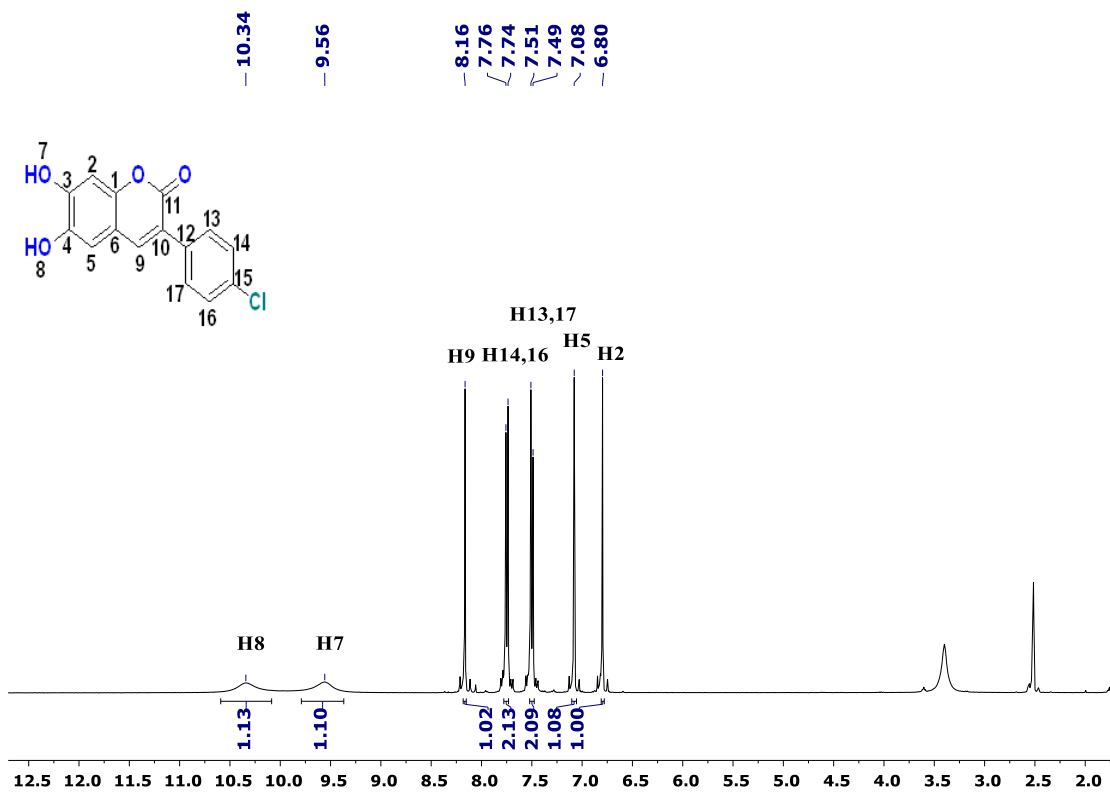
Figure S5. ^{1}H NMR spectrum of the probe **MCPC** in DMSO–d_6

Figure S6. ^{13}C–APT NMR spectrum of the probe **MCPC** in DMSO–d_6
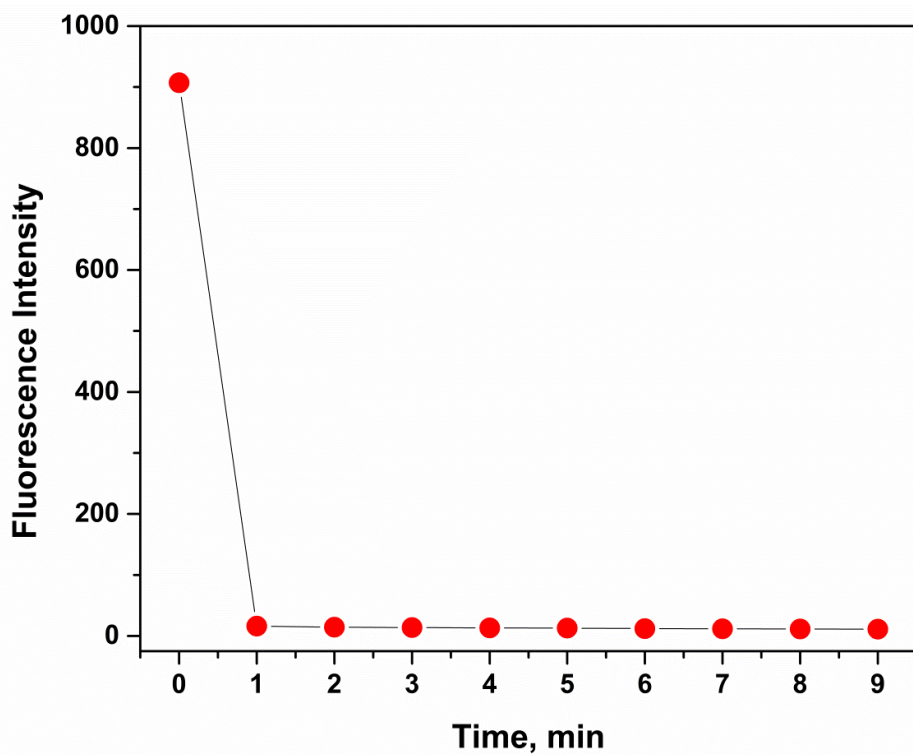
Figure S7. Response time of the **MCPC–Cu^{2+}** complex
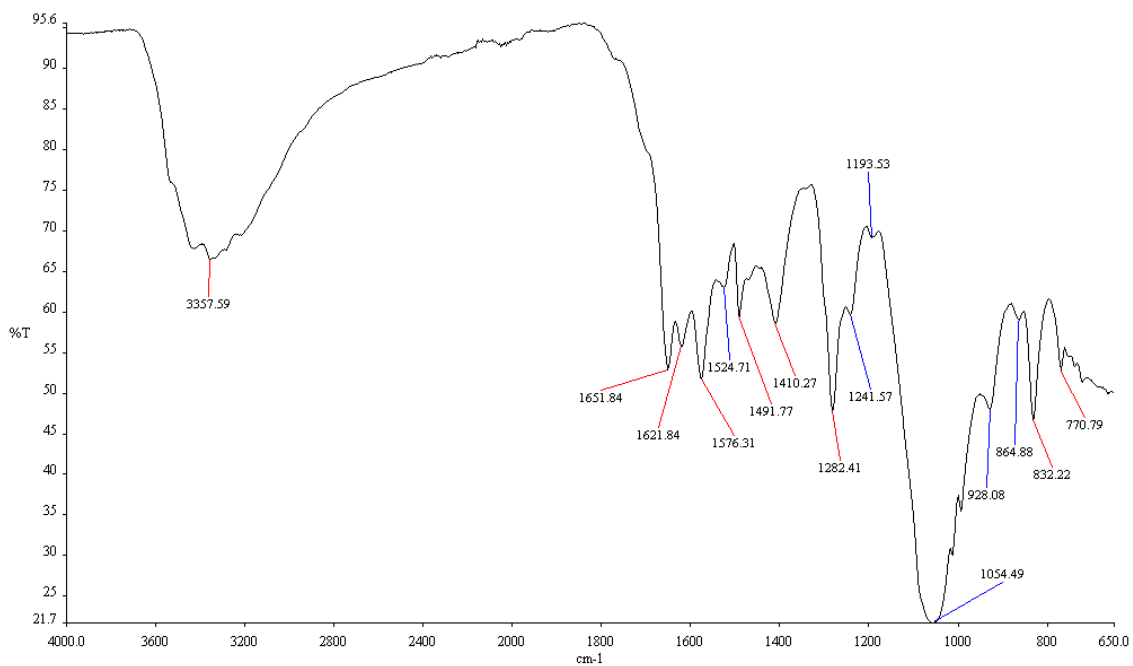
Figure S8. FT–IR spectrum of the **MCPC–Cu^{2+}** complex

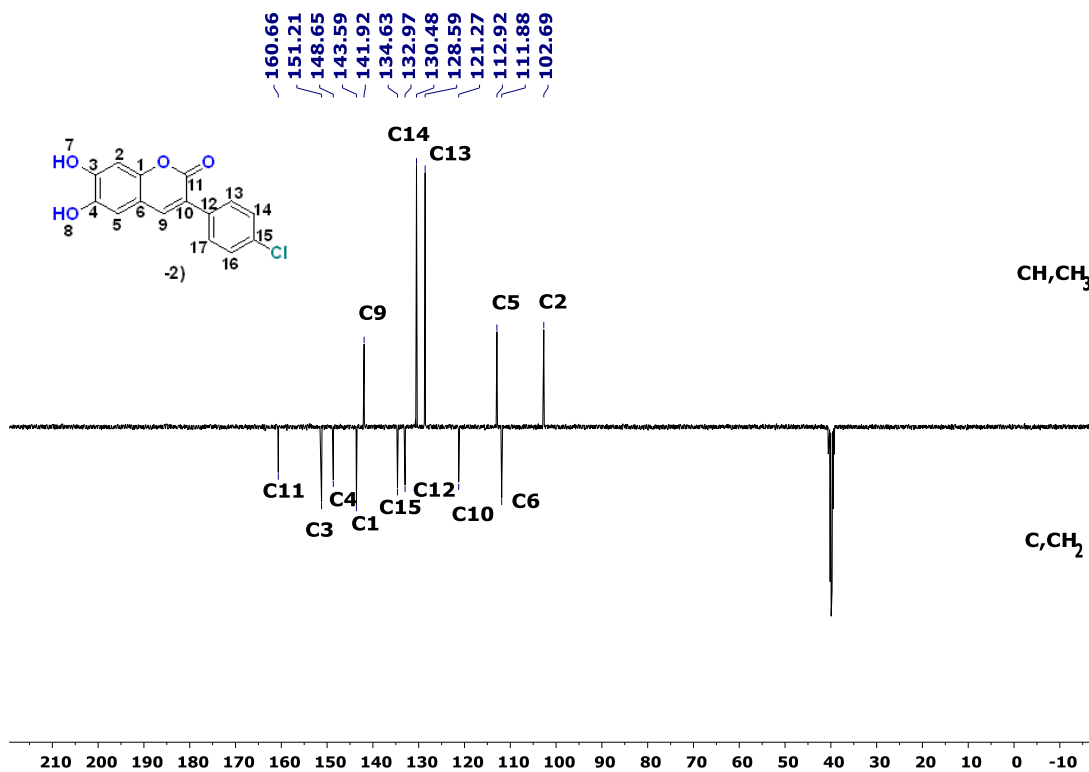**Table S1**. Operating parameters for the ICP–OES analysis

parameter	setting
Plasma torch:	standard one piece quartz axial, one–piece with 2.4 mm injector
Spray chamber type:	glass cyclonic (single–pass)
Supplied rf power:	1.0 kW
Plasma Ar gas flow:	10 L.min^{-1}
Auxiliary Ar gas flow:	1.0 L.min^{-1}
Nebulizer Ar gas flow:	0.85 L.min^{-1}
Nebulizer type:	sea spray
Pump tubing Rinse/Instrument pump:	white–white tabs (1.02 mm id) – Waste: blue–blue tabs (1.65 mm id)
Pump speed:	20 rpm
Total sample usage:	1 mL
Replicate read time:	15 sec
Number of replicates:	5
Sample uptake delay time:	20 sec
Stabilization time:	10 sec
Rinse time:	10 sec
Fast pump:	on
Wavelengths from 167 to 785 nm	Cu 324.754 nm, Cd 228.8 nm, Hg 253.7 nm, Zn 213.8 nm, Pb 405.8 nm, Ag 328.1 nm, and Tl 377.6 nm

Table S2. Determination of Cu^{2+} in herbal and black tea samples by the probe **MCPC**

sample	Cu^{2+} added ($\mu mol\ L^{-1}$)	Cu^{2+} found ($\mu mol\ L^{-1}$)	recovery (%)	RSD (%) (n=3)
herbal tea samples				
green tea	0.00	0.17 ±0.002		1.20
	0.10	0.27 ±0.003	100.65	0.92
	0.20	0.37 ±0.002	99.28	0.56
green tea (mixed with rose)	0.00	0.02 ±0.0004		1.75
	0.10	0.12 ±0.002	91.64	1.31
	0.20	0.23 ±0.003	104.42	1.38
white tea	0.00	0.13 ±0.001		0.80
	0.10	0.22 ±0.002	93.41	0.90
	0.20	0.32 ±0.002	99.52	0.81
sage tea	0.00	0.07 ±0.0001		1.22
	0.10	0.16 ±0.001	93.63	0.61
	0.20	0.29 ±0.002	108.23	0.73
fennel tea	0.00	0.04 ±0.0004		1.04
	0.10	0.13 ±0.001	90.22	0.59
	0.20	0.24 ±0.003	101.25	0.98
daisy tea	0.00	0.08 ±0.001		1.06
	0.10	0.18 ±0.003	98.36	1.41
	0.20	0.27 ±0.004	96.10	1.29
rose hip tea	0.00	0.07 ±0.001		1.48
	0.10	0.17 ±0.002	105.78	0.88
	0.20	0.25 ±0.003	91.70	1.00
ginger tea	0.00	0.02 ±0.0002		1.03
	0.10	0.11 ±0.001	91.79	0.88
	0.20	0.22 ±0.001	98.73	0.50
mint tea	0.00	0.09 ±0.001		1.16
	0.10	0.19 ±0.001	102.17	0.27
	0.20	0.27 ±0.004	93.16	1.57
apple tea	0.00	0.01 ±0.0001		0.97
	0.10	0.12 ±0.002	106.51	1.31
	0.20	0.21 ±0.001	101.06	0.47
linden tea	0.00	0.09 ±0.001		1.07
	0.10	0.20 ±0.001	109.19	0.50
	0.20	0.30 ±0.002	104.17	0.51
black tea samples				
black tea without aroma–A	0.00	0.08 ±0.001		1.19
	0.10	0.19 ±0.001	100.80	0.40
	0.20	0.29 ±0.001	102.63	0.35
black tea without aroma–B	0.00	0.02 ±0.0002		1.38
	0.10	0.12 ±0.002	100.82	1.28
	0.20	0.23 ±0.003	108.37	1.14
black tea without aroma–C	0.00	0.05 ±0.0002		0.65
	0.10	0.14 ±0.002	90.47	1.39
	0.20	0.27 ±0.003	108.92	0.93
black tea with bergamot aroma–A	0.00	0.13 ±0.001		0.65
	0.10	0.23 ±0.002	101.35	0.65
	0.20	0.34 ±0.003	104.06	0.90
black tea with bergamot aroma–B	0.00	0.05 ±0.0003		0.53
	0.10	0.15 ±0.001	99.55	0.77
	0.20	0.23 ±0.003	91.02	1.29

Table S3. Determination of Cu^{2+} in herbal and black tea samples by **ICP–OES**

sample	Cu^{2+} added ($\mu g\ L^{-1}$)	Cu^{2+} found ($\mu g\ L^{-1}$)	recovery (%)	RSD (%) (n=3)
herbal tea samples				
green tea	0	10.96 ±0.11		0.96
	10	20.55 ±0.16	95.96	0.78
	20	30.72 ±0.13	98.83	0.43
green tea (mixed with rose)	0	1.16 ±0.04		2.44
	10	11.46 ±0.10	98.77	0.85
	20	21.67 ±0.38	100.27	1.74
white tea	0	8.11 ±0.11		1.35
	10	17.88 ±0.112	97.67	0.70
	20	27.76 ±0.17	98.28	0.61
sage tea	0	4.34 ±0.09		1.98
	10	14.45 ±0.06	101.11	0.44
	20	24.23 ±0.13	99.48	0.55
fennel tea	0	2.45 ±0.05		1.96
	10	12.16 ±0.05	97.08	0.40
	20	22.48 ±0.15	100.14	0.67
daisy tea	0	5.02 ±0.06		1.28
	10	15.15 ±0.16	101.39	1.05
	20	25.52 ±0.22	102.50	0.87
rose hip tea	0	4.21 ±0.08		1.87
	10	14.11 ±0.10	99.08	0.69
	20	24.42 ±0.46	101.09	1.88
ginger tea	0	1.40 ±0.07		4.97
	10	11.25 ±0.06	98.52	0.56
	20	20.90 ±0.07	97.50	0.33
mint tea	0	5.43 ±0.11		2.00
	10	16.00 ±0.03	105.66	0.20
	20	25.39 ±0.27	99.81	1.07
apple tea	0	0.65 ±0.04		5.76
	10	10.44 ±0.10	97.97	0.93
	20	19.56 ±0.06	94.58	0.32
linden tea	0	5.57 ±0.08		1.48
	10	15.59 ±0.06	100.27	0.41
	20	24.87 ±0.10	96.53	0.39
black tea samples				
black tea without aroma–A	0	5.37 ±0.14		2.68
	10	14.82 ±0.05	94.46	0.32
	20	25.34 ±0.06	99.84	0.25
black tea without aroma–B	0	1.08 ±0.04		3.35
	10	11.44 ±0.10	103.66	0.83
	20	20.93 ±0.17	99.30	0.80
black tea without aroma–C	0	3.41 ±0.08		2.43
	10	13.30 ±0.13	98.84	0.96
	20	23.50 ±0.30	100.43	1.29
black tea with bergamot aroma–A	0	8.38 ±0.19		2.32
	10	17.91 ±0.10	95.33	0.54
	20	27.78 ±0.19	97.01	0.70
black tea with bergamot aroma–B	0	3.31 ±0.13		3.90
	10	13.46 ±007	101.41	0.54
	20	23.73 ±0.26	102.05	1.08

References

1.   Ozen F, Tekin S, Koran K, Sandal S, Gorgulu AO. Synthesis, structural characterization, and in vitro anti-cancer activities of new phenylacrylonitrile derivatives. Applied Biological Chemistry 2016; 59 (1): 239-248. doi: 10.1007/s13765-016-0163-x

2.   Buu-Hoi NP, Saint-Ruf G, Lobert B. Oxygen heterocycles. part XIV. hydroxylated 3-awl- and 3-pyridyl-coumarins. Journal of the Chemical Society C: Organic 1968; 16 (1): 2069-2070. doi: 10.1039/J39690002069

3.   Elgazzar E, Dere A, Özen F, Koran K, Al-Sehemi AG et al. Design and fabrication of dioxyphenylcoumarin substituted cyclotriphosphazene compounds photodiodes. Physica B: Condensed Matter 2017; 515 (1): 8-17. doi: 10.1016/j.physb.2017.03.025